Neurobiology of Aging 69 (2018) 94–101

Contents lists available at ScienceDirect

Neurobiology of Aging

journal homepage: www.elsevier.com/locate/neuaging

Levels of retinal IAPP are altered in Alzheimer's disease patients and correlate with vascular changes and hippocampal IAPP levels

Nina Schultz [a], Elin Byman [a], The Netherlands Brain Bank [b], Malin Wennström [a,*]

[a] Clinical Memory Research Unit, Department of Clinical Sciences Malmö, Lund University, Malmö, Sweden
[b] Netherlands Institute for Neuroscience, Amsterdam, The Netherlands

ARTICLE INFO

Article history:
Received 27 February 2018
Received in revised form 6 April 2018
Accepted 2 May 2018
Available online xxx

Keywords:
Alzheimer's disease
Hippocampus
IAPP
Pericytes
Retina

ABSTRACT

Islet amyloid polypeptide (IAPP) forms toxic aggregates in the brain of patients with Alzheimer's disease (AD). Whether IAPP also affects the retina in these patients is still unknown. Levels of IAPP in soluble and insoluble homogenate fractions of retina and hippocampus from AD patients and nondemented controls were analyzed using ELISA. Number of pericytes and vessel length were determined by analysis of immunostained retina and hippocampus. Insoluble retinal fractions of AD patients contained lower levels of unmodified IAPP, whereas soluble retinal fractions contained increased levels of the same. Total IAPP levels and pericyte numbers in retina mirrored corresponding variables in the hippocampus. Moreover, levels of total unmodified IAPP correlated negatively with the vessel length both in retina and hippocampus across the group and positively with pericyte numbers in retina in AD patients. Our studies indicate that changes in brain IAPP are reflected by corresponding levels in the retina. Our results also suggest modification of IAPP as an important event implicated in vascular changes associated with AD.

1. Introduction

In addition to amyloid beta (Aβ), recent studies have suggested yet another amyloid peptide forming plaques in the brain of patients with Alzheimer's disease (AD) (Jackson et al., 2013; Oskarsson et al., 2015). This peptide is called islet amyloid polypeptide (IAPP) and is mostly known for its role in type 2 diabetes (T2D) pathology. The biological function of IAPP is to regulate degradation of food in the stomach and thereby release of glucose to the blood. IAPP readily crosses the blood-brain barrier into the brain, where it is known to regulate appetite (Banks et al., 1995). However, studies implicate that IAPP may also play a role in cognitive function. Indeed, treatment with IAPP or its analog pramlintide, have shown to improve cognitive functions and reduce AD pathology in transgenic AD mice (Adler et al., 2014; Zhu et al., 2014). In addition, a positive association between unmodified plasma IAPP and cognition (Qiu et al., 2014) as well as decreased levels of unmodified plasma IAPP in AD patients have been reported (Adler et al., 2014). A regulatory role of IAPP on Aβ accumulation has also been suggested as peripheral injections of IAPP or pramlintide increase the translocation of Aβ from the brain into the blood (Zhu et al., 2014). Yet, if IAPP becomes modified (either by reduction of the C2-C7 disulphide bond or by C-terminal deamidation), it loses its biological activity and starts to aggregate into cell toxic depositions. These depositions are commonly found in heart tissue (Despa et al., 2012), kidney (Gong et al., 2007), and pancreas of patients with T2D (Westermark et al., 2011). Interestingly, studies have also shown the presence of IAPP depositions, occasionally together with Aβ, in the brain of AD patients (Jackson et al., 2013; Oskarsson et al., 2015). Moreover, oligomerized IAPP in plasma from AD patients has been proposed as a mechanism underlying the IAPP accumulation in the brain (Jackson et al., 2013). We have, by the use of postmortem human tissue studies and in vitro studies, demonstrated that IAPP is internalized by vessel-supporting brain pericytes and forms toxic inclusions (Schultz et al., 2016)—a finding interesting from the perspective that pericyte loss has been demonstrated in AD patients (Sengillo et al., 2013).

Even though AD is a neuropathological disease, several studies point toward the occurrence of pathological changes also in other organs of these patients. The eye is such an organ and because the retina is both anatomically and developmentally known as an extension of the brain (London et al., 2013), analysis of the retina has become increasingly interesting within the research field of AD. Studies highlight retinal imaging as a potential noninvasive method to diagnose AD, where the retina serves as a type of window to study pathological changes in the brain. For example,

* Corresponding author at: Clinical Memory Research Unit, Department of Clinical Sciences Malmö, Inga Marie Nilssonsgata 53, 205 02 Malmö, Sweden. Tel.: +46 40 335733; fax: +46 40 391004.
E-mail address: malin.wennstrom@med.lu.se (M. Wennström).

https://doi.org/10.1016/j.neurobiolaging.2018.05.003

depositions of Aβ in the retina correlate with AD severity (Koronyo-Hamaoui et al., 2011), thinning of blood vessels and reduced flow rates are observed in early AD patients (Hinton et al., 1986; Ratnayaka et al., 2015), and vascular alterations in retina have been shown to correlate with the burden of cerebral Aβ in these patients (Frost et al., 2013). The link between retina and brain is furthermore demonstrated by studies showing retinal arteriolar abnormalities along with cerebral white-matter lesions (indicating vascular damage) (Kwa et al., 2002). Whether IAPP, in similarity to Aβ, is present or deposits in the retina has not (to our knowledge) been described before. Thus, to investigate whether IAPP can be found in the retina, we here analyze IAPP levels in different fractions of retinal and hippocampal homogenates from AD patients and nondemented controls (NCs). To further follow up our previous studies on IAPP and brain pericytes (Schultz et al., 2016), we also study the association between IAPP levels and changes in the retinal and hippocampal vasculature/pericyte population. Finally, we investigate whether the retina mirrors the hippocampal changes in regard to IAPP levels, pericyte population and vessel length.

2. Methods

2.1. Individuals included in the study

Frozen samples of retina (right eyeball) and midlevel hippocampus from clinically verified and postmortem-verified patients with AD (n = 12) and NCs (n = 8) from the Netherlands Brain Bank were included in the study. Two individuals (n = 1 NC, n = 1 AD patient) were diagnosed with diabetes mellitus type II. Apolipoprotein E (APOE) genotype, demographic data, and neuropathological assessment (Braak and ABC stages) are presented in Table 1. Written consent for the use of tissue and clinical data for research purposes was obtained from all patients or their next of kin in accordance with the International Declaration of Helsinki. The medical ethics review committee of VU medical center, Amsterdam, has approved the procedures of tissue collection, and the regional ethical review board in Lund has approved the study. All human data were analyzed anonymously.

2.2. Tissue extraction

Retina samples (1.0 × 0.5 cm) and hippocampal samples (CA1 and molecular layer) (approximately 30 mg), were homogenized in 100% formic acid (FA) (10 μL/mg tissue), incubated over night at room temperature (RT), centrifuged at 13.000 × *g* for 20 minutes 4 °C and the supernatant was then collected, lyophilized, and redissolved in dimethyl sulfoxide to generate the supernatant from low-speed centrifuged FA-treated homogenate ($S_{L\text{-}FA}$) fraction. To generate the ultracentrifuged FA-treated homogenate ($S_{U\text{-}FA}$), pellet from ultracentrifuged FA-treated homogenate ($P_{U\text{-}FA}$), and pellet from ultracentrifuged FA-treated homogenate treated with guanidine hydrochloride ($P_{U\text{-}FA\text{-}G}$) fraction, retina and hippocampal samples were homogenized in cell lysis buffer (Sigma Aldrich, St. Louis, MO) together with protease inhibitors at 4 °C and ultracentrifuged 350.000 × *g* for 1 hour at 4 °C. The supernatant ($S_{U\text{-}FA}$) was collected, and the pellet was rehomogenized in 100% FA (10 μL/mg tissue), incubated 1 hour at RT, and then centrifuged at 13.000 × *g* for 20 minutes at 4 °C. The supernatant was lyophilized and then either redissolved in dimethyl sulfoxide to generate the $P_{U\text{-}FA}$ fraction or further incubated in 3M guanidine hydrochloride (GuHCl) (Millipore, Darmstadt, Germany) in tris -buffered saline for 2 hours at RT ($P_{U\text{-}FA\text{-}G}$).

2.3. Analysis of IAPP levels

Levels of unmodified IAPP in the $S_{L\text{-}FA}$, $S_{U\text{-}FA}$, and $P_{U\text{-}FA}$ fractions were analyzed using Human Amylin ELISA kit (Millipore) according to manufacturer's instructions. The total IAPP levels (i.e., unmodified and modified) in the $P_{U\text{-}FA\text{-}G}$ fraction were analyzed using an in-house–developed direct ELISA. An antibody directed against the (20–29) sequence of IAPP (Paulsson and Westermark, 2005) (rabbit anti-IAPP A133, kind gift from Professor Gunilla Westermark, Uppsala University) was used as detection antibody. Samples, positive control (IAPP peptide, Bachem, Bubendorf, Switzerland) and negative control (Aβ peptide, AlexoTech AB, Umeå, Sweden) were incubated at 4 °C over night. The following day, the plate was incubated with blocking solution (BS) (1% bovine serum albumin in phosphate-buffered saline) 1 hour at RT, primary antibody 2 hours at RT on shaker and finally goat-anti-rabbit horseradish peroxidase

Table 1
Demographic data, apolipoprotein E (APOE) genotype, neuropathological assessment of individuals included in the study

Clinical diagnosis	Gender	Age (y)	Neuropat. Ev (NFT/Aβ/LB)	APOE genotype	Cause of death
NC	M	70	1/0/3	3/2	Pneumonia with cardiogenic shock
NC	M	55	0/0/0	3/3	Euthanasia, esophageal cancer
NC	M	75	1/A/0	3/3	Cardiac arrest with COPD
NC	F	60	0/0/0	3/2	Metastasized mama carcinoma
NC	F	84	2/B/0	3/3	Pulmonary dysfunction
NC	M	81	3/C/0	4/3	Terminal pancreas carcinoma
NC	M	102	3/A/0	4/3	Ileus
NC	F	92	3/0/1	4/3	Heart failure
AD	M	96	4/C/0	3/3	Cardiac arrest
AD	F	69	4/B/0	3/3	Heart failure
AD	F	83	4/C/6	3/3	Gastro-enteritis, dementia
AD	F	88	5/C/5	3/3	Cachexia, vascular dementia
AD	M	92	6/C/0	4/3	Pneumonia
AD	F	88	5/C/1	4/3	Dehydration, dementia
AD	F	85	5/C/0	4/3	Pneumonia/palliative sedation
AD	F	70	6/C/0	4/3	Atrioventricular block, severe AD
AD	F	91	6/C/0	4/4	Cachexia, advanced dementia
AD	F	64	4/C/0	4/4	Euthanasia, AD
AD	F	78	6/C/0	3/3	Dehydration, cachexia, AD
AD	M	63	4/C/6	4/4	Hepatic insufficiency, metastases

Individuals clinically diagnosed with Alzheimer's disease (AD) and nondemented controls (NC) are included in the study. Braak staging of neurofibrillary tangles (NFT) and Lewy bodies (LBs) and ABC staging of amyloid (Aβ).
Key: F, female; M, male; Neuropat. Ev, neuropathological evaluation.

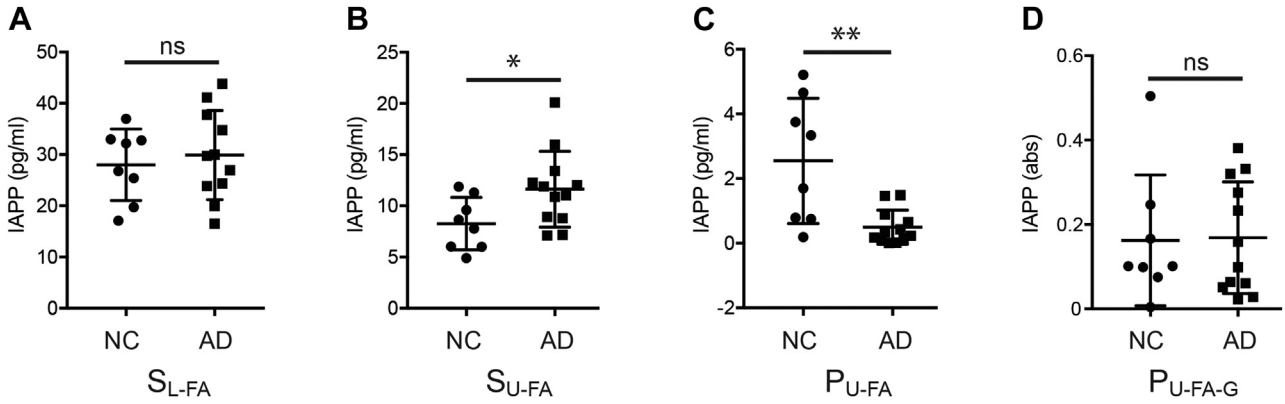

Fig. 1. Column scatterplots demonstrate differences in mean IAPP levels in different fractions (S_{L-FA}, S_{U-FA}, P_{U-FA}, and P_{U-FA-G}) in retinas of nondemented controls (NCs) and patients with Alzheimer's disease (AD). (A) Column scatterplot demonstrates no significant differences in S_{L-FA} between AD patients and the NC group. (B) Column scatterplot demonstrates significantly higher levels of IAPP in the S_{U-FA} fraction in AD patients compared with NCs. (C) Column scatterplot shows significantly lower levels of IAPP in the P_{U-FA} fraction in AD patients compared with NCs. (D) Column scatterplot demonstrates no significant difference in IAPP levels in the P_{U-FA-G} fraction between AD patients and the NC group. Data are analyzed using student *t*-test, and values are presented as means ± standard deviations. * Significant difference at $p < 0.05$ level ** Significant difference at $p < 0.01$ level. Abbreviations: IAPP, islet amyloid polypeptide; P_{U-FA}, pellet from ultracentrifuged formic acid–treated homogenate; P_{U-FA-G}, pellet from ultracentrifuged formic acid–treated homogenate treated with guanine hydrochloride; S_{L-FA}, supernatant from low-speed centrifuged formic acid–treated homogenate; S_{U-FA}, supernatant from ultracentrifuged formic acid–treated homogenate.

secondary antibody (Santa Cruz Biotechnology, Santa Cruz, CA) 1 hour at RT on shaker. The intra- and inter-assay variation coefficient (CV%) were <9 and <10, respectively. Total IAPP was also analyzed using dot blot. The samples (0.5 μg/μL, 2 μL) of the P_{U-FA-G} fraction were loaded into nitrocellulose membranes and let dry 30 minutes before blocking the membranes with 5% milk phosphate-buffered saline-Tween 20 1 hour at RT and incubation with A133 (1:1000) in BS ON at 4 °C. The following day the membranes were incubated with goat-anti-rabbit horseradish peroxidase (1:10,000, Abcam, Cambridge, UK) for 1 hour at RT. Digitalized images of dot blots were used to quantify protein levels based on optical density (Image Lab Software [BioRad, Hercules, CA]).

2.4. Immunostaining

Retina (1.0 × 0.5 cm) was cut 0.5 cm from the optic nerve in the far peripheral superior part of the eye and fixed in 4% paraformaldehyde for 4 hours. The hippocampal tissue was fixed in 4% paraformaldehyde for 4 hours before sectioned in 40-μm thick sections. The retinal and hippocampal tissue was stained against NG2 (MAB2029; Millipore) using immunofluorescence and immunohistochemistry, respectively, according to previously published protocols (Schultz et al., 2016). The number of NG2-positive pericytes and the length of the vessels in retina and the hippocampal molecular layer were analyzed by a blinded observer and measured using an Olympus AX70 light microscope equipped with 20× objectives and ImageJ. Pictures (Olympus cellSens Dimension) of 2 randomly chosen fields (345 × 440 mm) of 3 sections (6 fields in total) from each individual were scored and measured. The number of NG2-positive pericytes/vessel length was thereafter calculated.

2.5. Statistical analysis

Statistical analysis was performed using SPSS software 24.0 (SPSS Inc, Chicago, IL). The Kolmogorov–Smirnov test was used to assess normal distribution. Differences were analyzed by the use of independent-samples *t*-test. Correlations between the investigated variables were examined using 2-tailed Pearson correlation test or 2-tailed Spearman correlation test. Results are presented as means ± standard deviation. A $p < 0.05$ was considered significant.

3. Results

3.1. Levels of unmodified IAPP in retinal and hippocampal fractions

We initiated our studies by analyzing levels of unmodified IAPP levels in 3 different fractions of retinal and hippocampal tissue from NCs and AD patients. The first fraction constituted the supernatant (S) from low-speed (L) centrifuged formic acid (FA) treated homogenate (S_{L-FA}), and therefore contains most of the IAPP (soluble and insoluble) found in the retina/hippocampal samples. The second fraction constituted the supernatant (soluble IAPP) from ultra-centrifuged formic acid treated homogenate (S_{U-FA}). Finally, the third fraction (P_{U-FA}) constituted the pellet (insoluble IAPP) from ultra-centrifuged formic acid treated homogenate. Analysis of the S_{L-FA} fraction showed no significant differences in IAPP levels between AD patients and NCs in either retina (Fig. 1A, Table 2) or hippocampal tissue (Table 2). However, we found significantly higher retinal IAPP levels in the S_{U-FA} fraction from AD

Table 2
Islet amyloid polypeptide levels in different fractions of retina and hippocampus samples

Fraction	NC	AD
Retina S_{L-FA} (pg/mL)	27.99 ± 6.98	29.89 ± 8.71
Retina S_{U-FA} (pg/mL)	8.27 ± 2.55	11.63 ± 3.70*
Retina P_{U-FA} (pg/mL)	2.55 ± 1.93	0.50 ± 0.53**
Retina P_{U-FA-G} (abs) ELISA	0.16 ± 0.16	0.17 ± 0.13
Retina PU-FA-G (abs) dot blot	152,348.46 ± 154825.96	120,313.24 ± 135,344.56
Brain SL-FA (pg/mL)	14.14 ± 10.59	15.20 ± 7.33
Brain SU-FA (pg/mL)	4.53± 1.56	3.27 ± 1.58
Brain PU-FA (pg/mL)	1.50 ± 1.72	0.81 ± 0.83
Brain PU-FA-G (abs) ELISA	0.03 ± 0.04	0.03 ± 0.02
Brain PU-FA-G (abs) dot blot	37,838.51 ± 39,860.23	36,674.48 ± 46,046.35

Retinas and hippocampi from individuals clinically diagnosed with Alzheimer's disease (AD) and nondemented controls (NC) included in the study. Mean values of IAPP ± standard deviation in the 4 different fractions (S_{L-FA}, S_{U-FA}, P_{U-FA}, and P_{U-FA-G}) of retinal and hippocampal tissue.
Key: IAPP, islet amyloid polypeptide; P_{U-FA}, pellet from ultracentrifuged formic acid–treated homogenate; P_{U-FA-G}, pellet from ultracentrifuged formic acid–treated homogenate treated with guanine hydrochloride; S_{L-FA}, supernatant from low-speed centrifuged formic acid–treated homogenate; S_{U-FA}, supernatant from ultra-centrifuged formic acid–treated homogenate.
* Significant difference at $p > 0.05$ level. ** Significant difference at $p > 0.01$ level.

patients compared with NCs ($p = 0.038$) (Fig. 1B, Table 2). No significant differences were found between the 2 patient groups when analyzing the IAPP levels in the corresponding hippocampal fraction (Table 2). The retinal $P_{U\text{-}FA}$ fraction contained significantly lower IAPP levels in AD patients compared with NCs ($p = 0.002$) (Fig. 1C, Table 2). A similar trend was seen when analyzing the corresponding hippocampal fraction; however, this difference did not reach significance (Table 2). Levels of IAPP in the different retinal and hippocampal fractions did not differ significantly with regard to age, gender, or APOE-ε4 status (data not shown). Finally, because a portion of the individuals included in the study (NCs n = 2 and AD patients n = 4) displayed some alpha synucleinopathy (Lewy bodies [LBs]) (notably not in the hippocampus), we analyzed the values also after excluding patients with LBs. Similar results, regardless of fractions analyzed, were detected (data not shown). In addition, 2 individuals (NC n = 1 and AD patient n = 1) were diagnosed with T2D, and because T2D is associated with alterations in IAPP secretion (high in prediabetic stages and low in late diabetic stages), we also analyzed IAPP levels after excluding the T2D patients. Again, we found similar results (data not shown) with the exception that the former significance found in $S_{U\text{-}FA}$ now only remained as a tendency to significance ($p = 0.081$).

3.2. Levels of total IAPP in retinal and hippocampal fractions

Because we found lowered levels of unmodified IAPP in the $P_{U\text{-}FA}$ fraction from AD patients, we found it interesting to investigate whether these levels correspond to the total amount of IAPP in this fraction. Currently, there is no commercially available ELISA measuring total IAPP, and we therefore developed an in-house direct ELISA using an antibody (A133) detecting both unmodified and modified IAPP. In addition, as previous studies have shown that GuHCl enhances IAPP antigen exposure (Fowler et al., 2007; Peranen et al., 1993), we treated the $P_{U\text{-}FA}$ fraction with GuHCl ($P_{U\text{-}FA\text{-}G}$). When analyzing IAPP levels in the $P_{U\text{-}FA\text{-}G}$ fraction, we found no significant differences between AD patients and NCs in either retina (Fig. 1D, Table 2) or hippocampal tissue (Table 2). To verify our results, we additionally analyzed the $P_{U\text{-}FA\text{-}G}$ fraction using an IAPP dot blot protocol previously described by Despa et al., 2012. The dot blot analysis on retinal and hippocampal IAPP levels in $P_{U\text{-}FA\text{-}G}$ fraction yielded similar results as the corresponding ELISA analysis (Table 2). The retinal and hippocampal IAPP levels analyzed with both dot blot and ELISA did not differ significantly with regard to age, gender, or APOE-ε4 status (data not shown).

3.3. Correlations between IAPP levels in retina and hippocampus

Correlation analysis showed no significant correlations between retinal and hippocampal IAPP levels in the $S_{L\text{-}FA}$ fraction across the group ($r = 0.077$, $p = 0.760$). However, when the groups were analyzed separately, a positive correlation was detected in NCs ($r = 0.821$, $p = 0.023$) (Fig. 2A), but not in AD patients ($r = -0.364$, $p = 0.272$). Similarly, no correlation was found between retinal and hippocampal IAPP levels in the $P_{U\text{-}FA}$ fraction across the group ($r = -0.132$, $p = 0.698$), but a tendency toward a positive correlation was found in NCs ($r = 0.771$, $p = 0.072$) (Fig. 2B), but not in AD patients ($r = -0.300$, $p = 0.370$). We further found a positive correlation between retinal and hippocampal IAPP levels in the $P_{U\text{-}FA\text{-}G}$ fraction across the group ($r = 0.498$, $p = 0.042$) (Fig. 2C). When the 2 groups were analyzed separately, this positive correlation remained significant in AD patients ($r = 0.727$, $p = 0.011$) (Fig. 2C), but not in NCs ($r = -0.086$, $p = 0.872$). Similar correlations were found using dot blot analysis, both across the group ($r = 0.549$, $p = 0.022$) and between AD and NC groups ($r = 0.836$, $p = 0.001$ and $r = 0.029$, $p = 0.957$, respectively). We found no correlations between retinal and hippocampal IAPP levels in the $S_{U\text{-}FA}$ fraction, regardless of whether the whole cohort was analyzed or the 2 groups separately (data not shown).

3.4. Number of pericytes, vessel length, and number of pericytes/vessel in the retina and hippocampus

Analysis of the NG2-positive retinal pericyte population showed no significant differences in either number of pericytes, vessel length, or number of pericytes/vessel length between the 2 groups when the whole cohort was analyzed. When excluding patients with LB pathology, the number of pericytes was significantly lower in AD patients compared with NCs (12.75 ± 5.33 vs. 19.20 ± 4.79, $p = 0.038$) (Fig. 3A). We also found close to significantly fewer pericytes/vessel in AD patients compared with NCs (4.27 ± 1.67 vs. 6.27 ± 1.86, $p = 0.056$) (Fig. 3B), whereas no difference in the vessel length was found between the 2 groups (3.01 ± 0.37 vs. 3.15 ± 0.62, $p = 0.606$). Furthermore, no significant differences were found between any of the hippocampal pericyte variables when the whole cohort was analyzed. But when individuals with LB pathology were excluded, a tendency toward fewer hippocampal pericytes in AD patients compared with NCs was found (8.43 ± 4.40 vs. 11.86 ± 1.75, $p = 0.099$) (Fig. 3C), as well as significantly reduced hippocampal vessel length in AD patients compared with NCs (1.55 ± 0.45 vs. 2.08 ± 0.31, $p = 0.028$)

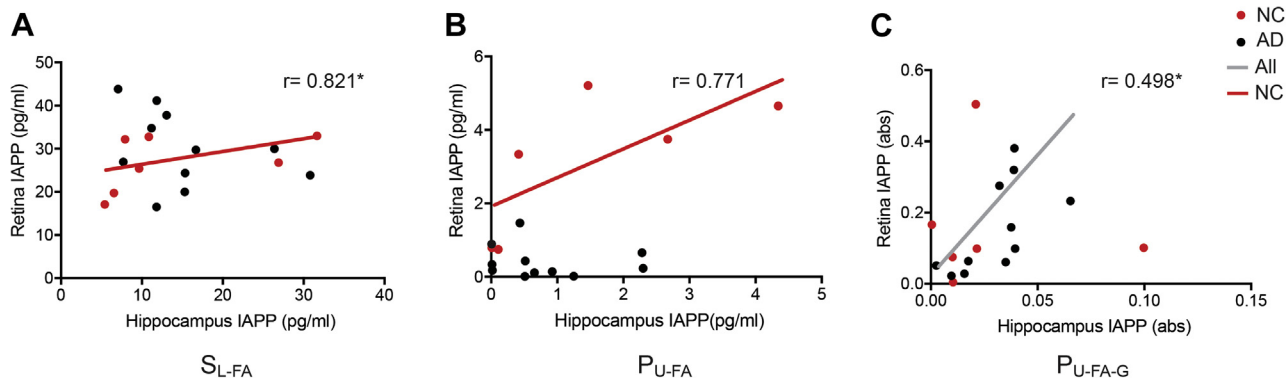

Fig. 2. Scatterplots and regression lines showing the associations between IAPP levels in different fractions of retinas and hippocampi of nondemented controls (NCs) (red dots, red line) and patients with Alzheimer's disease (AD) (black dots, black lines). (A) Scatterplot shows significant positive association between retinal and hippocampal IAPP levels in the $S_{L\text{-}FA}$ fraction in the NC group (red dots and red line). (B) Scatterplot demonstrates a tendency toward significant positive correlation between retinal and hippocampal IAPP levels in the $P_{U\text{-}FA}$ fraction in the NC group (red dots and red line). (C) Scatterplot shows significant positive correlation between retinal and hippocampal IAPP levels in the $P_{U\text{-}FA\text{-}G}$ fraction in both the whole cohort (gray line) and in the AD group (black dots). Data are analyzed using 2-tailed Spearman correlation test. * Significant correlation at $p < 0.05$ level. Abbreviations: IAPP, islet amyloid polypeptide; $P_{U\text{-}FA}$, pellet from ultracentrifuged formic acid–treated homogenate; $S_{L\text{-}FA}$, supernatant from low-speed centrifuged formic acid–treated homogenate. (For interpretation of the references to color in this figure legend, the reader is referred to the Web version of this article.)

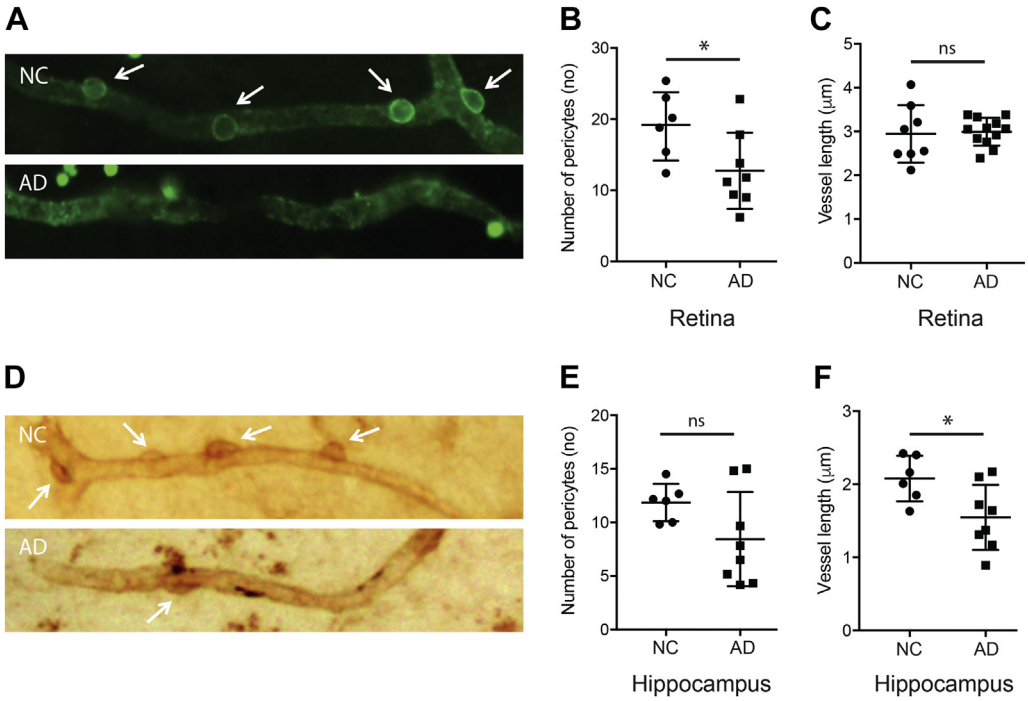

Fig. 3. Images show NG2-positive pericytes and vessels, and column scatterplots demonstrate differences in mean of pericyte variables (number of pericytes, vessel length, and number of pericytes/vessel) in retinal and hippocampal tissue of nondemented controls (NCs) and patients with Alzheimer's disease (AD) when excluding patients with LB pathology. (A) Representative images of NG2-positive pericytes and vessels in the retinas of NCs and AD patients. (B) Column scatterplot shows significantly lower number of retinal pericytes in AD patients compared with NCs. (C) Column scatterplot demonstrates a tendency toward lower number of retinal pericytes/vessel in AD patients compared with NCs. (D) Representative images of NG2-positive pericytes and vessels in the hippocampus of NCs and AD patients. (E) Column scatterplot shows a tendency toward lower number of hippocampal pericytes in AD patients compared with NCs. (F) Column scatterplot demonstrates significantly shorter hippocampal vessel length in AD patients compared with NCs. Data are analyzed using student *t*-test, and values are presented as means ± standard deviations. * Significant difference at $p < 0.05$ level.

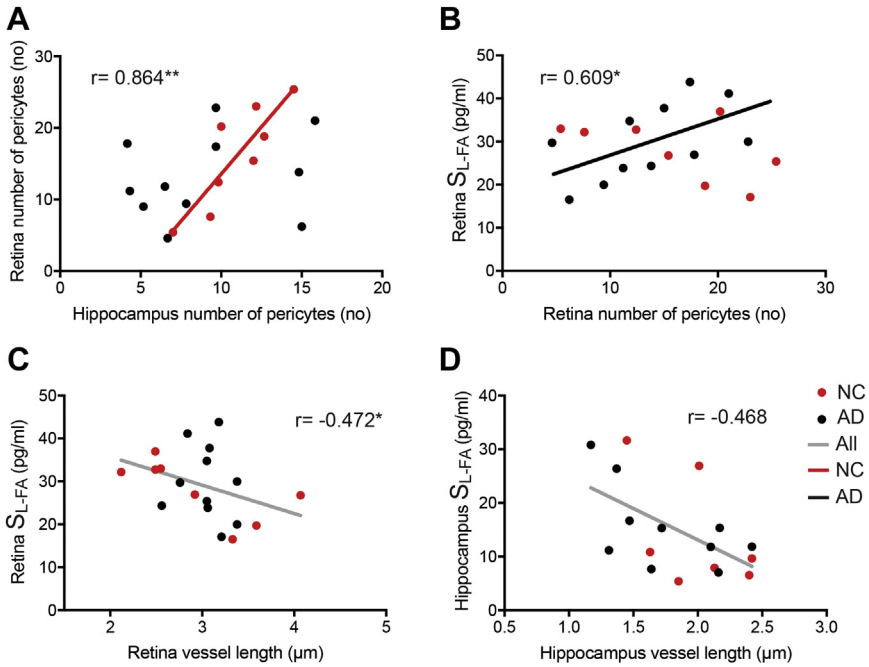

Fig. 4. Scatterplot and regression line showing the associations between the number of pericytes in retinas and hippocampi as well as the IAPP levels in the $S_{L\text{-}FA}$ fraction and the number of pericytes and vessel length in retinas and hippocampi of nondemented controls (NCs) (red dots) and patients with Alzheimer's disease (AD) (black dots) including patients with LB pathology. (A) Scatterplot demonstrates significant positive correlation between the number of pericytes in the retina and the number of pericytes in the brain in the NC group (red dots, red line). (B) Scatterplot shows significant positive association between IAPP levels in the $S_{L\text{-}FA}$ fraction and the number of pericytes in retina in AD patients (black line). (C) Scatterplot demonstrates significant negative correlation between IAPP levels in the $S_{L\text{-}FA}$ fraction and the vessel length in retina in the whole cohort (gray line). (D) Scatterplot shows significant negative association between IAPP levels in the $S_{L\text{-}FA}$ fraction and the vessel length in hippocampus in the whole cohort (gray line). Data are analyzed using 2-tailed Spearman correlation test. * Significant correlation at $p < 0.05$ level. ** Significant correlation at $p > 0.01$ level. Abbreviations: IAPP, islet amyloid polypeptide; LB, Lewy body; $S_{L\text{-}FA}$, supernatant from low-speed centrifuged formic acid–treated homogenate. (For interpretation of the references to color in this figure legend, the reader is referred to the Web version of this article.)

(Fig. 3D). No significant difference in number of pericytes/vessel length was found between the 2 groups (data not shown).

No significant differences in pericyte numbers, vessel length, or number of pericytes/vessel length were found with regard to age, gender, or APOE-ε4 status (data not shown).

3.5. Correlations between in retinal and hippocampal pericyte and vessel variables

Correlation analysis showed a tendency toward a positive correlation between the number of pericytes in the retina and in the hippocampus across the group ($r = 0.423$, $p = 0.071$) (Fig. 4A). When the 2 groups were analyzed separately, a significant positive correlation was found between the number of pericytes in retina and hippocampus in NCs ($r = 0.864$, $p = 0.006$) (Fig. 4A) but not in AD patients ($r = 0.213$, $p = 0.529$). No significant correlations between retina and hippocampus in regards to vessel length and number of pericytes/vessel length were found either across or between the groups (data not shown).

3.6. Correlations between IAPP levels and pericyte/vessel variables in the retina and hippocampus

Finally, we wanted to study the relationship between IAPP levels and pericyte/vessel variables. Correlation analysis showed no significant correlation between the number of retinal pericytes and retinal IAPP levels in the $S_{L\text{-}FA}$ fraction across the group ($r = 0.054$, $p = 0.825$). However, when the 2 groups were analyzed separately, a positive correlation was found in AD patients ($r = 0.609$, $p = 0.047$) (Fig. 4B), but not in NCs ($r = -0.524$, $p = 0.183$). We also found a significant negative correlation between retinal vessel length and retinal IAPP levels in the $S_{L\text{-}FA}$ fraction across the group ($r = -0.472$, $p = 0.041$) (Fig. 4C). This correlation remained only as a tendency in NCs ($r = -0.667$, $p = 0.071$) and was lost in AD patients ($r = -0.182$, $p = 0.593$) when the groups were analyzed separately. Correlation analysis was also performed between the remaining retinal IAPP fractions and measured pericyte variables, but no correlations were found either when the analysis was performed across the group or separately (data not shown). A tendency toward a negative correlation between hippocampal vessel length and hippocampal IAPP levels in the $S_{L\text{-}FA}$ fraction was found across the group ($r = -0.468$, $p = 0.058$), but when the 2 groups were analyzed separately, a significant positive correlation was found only between the number of hippocampal pericytes/vessel and IAPP levels in the $P_{U\text{-}FA\text{-}G}$ fraction in NCs ($r = 0.886$, $p = 0.019$) (Fig. 4D) but not in AD patients ($r = 0.139$, $p = 0.701$). No significant correlations were found between any of the hippocampal IAPP fractions and the number of hippocampal pericytes or number of hippocampal pericytes/vessel (data not shown).

4. Discussion

Depositions of IAPP have been found in various peripheral organs of patients with T2D (Jackson et al., 2013), and recent studies have shown depositions in the AD brain also (Jackson et al., 2013; Oskarsson et al., 2015). In this study, we demonstrate for the first time that IAPP also can be found in the human retina of NCs and AD patients. This finding may, at least in theory, not come as a surprise as the peptide is transported by the blood and therefore could be present in all tissues, including the highly vascularized eye. Interestingly, we found significantly higher levels of unmodified IAPP in the soluble retinal fraction ($S_{U\text{-}FA}$), but significantly lower levels of unmodified IAPP in the insoluble fraction ($P_{U\text{-}FA}$), in AD patients compared with NCs. Although, the significance of these findings remains elusive, it is instructive to remember that IAPP has to remain unmodified to bind to receptors and keep its biological activity (Jeong and An, 2015). In addition, IAPP is known to translocate Aβ from the brain over the blood-brain barrier to the blood (Zhu et al., 2014). Thus, it may be that the increased levels of unmodified soluble IAPP reflect a compensatory process aiming to enhance Aβ clearance in the AD brain. Another possible explanation can be found in the property of Aβ to competitively bind to the IAPP receptor (Fu et al., 2012; Zhu et al., 2014). Thus, increased levels of Aβ in AD patients could reduce IAPP binding to the receptor, consequently leading to reduced activation of IAPP-related signaling pathways as well as increased levels of soluble unbound IAPP. This hypothesis is further supported by the lowered levels of unmodified biologically active IAPP in the insoluble fraction of AD retina. The latter result, in combination with the unaltered total (unmodified and modified) IAPP levels found in the GuHCl-treated insoluble AD fraction, further suggests that AD patients have higher levels of modified IAPP compared with NCs. This idea needs however to be confirmed by an assay that separately measures modified IAPP. Such method is currently not available.

Modification of IAPP leads to an instable peptide that can seed unmodified and modified IAPP (Dunkelberger et al., 2012; Jeong and An, 2015) as well as Aβ and thereby form toxic aggregates in the AD brain (Jackson et al., 2013; Oskarsson et al., 2015). The aggregates may underlie the 1.4 times higher IAPP concentrations previously found in an insoluble FA-treated fraction of AD brains compared with control brains (Oskarsson et al., 2015). However, we could not detect any differences in either soluble or insoluble unmodified IAPP ($S_{L\text{-}FA}$, $S_{U\text{-}FA}$, $P_{U\text{-}FA}$) or insoluble total IAPP ($P_{U\text{-}FA\text{-}G}$) in the hippocampal fraction. This contradictory result may be due to differences in sample preparation and/or analysis method.

Our correlations analysis of retinal and hippocampal IAPP values showed increased levels of unmodified retinal IAPP, both soluble ($S_{L\text{-}FA}$) and insoluble ($P_{U\text{-}FA}$), along with increased levels of the same in hippocampus of NCs. Conversely, total retinal IAPP in the insoluble fraction ($P_{U\text{-}FA\text{-}G}$) increased in concert with increased total hippocampal IAPP specifically in AD patients. In view of these results, we speculate that the amount of unmodified IAPP in the retina only mirrors unmodified IAPP in the brain under healthy (nondemented) conditions. However, if the IAPP becomes modified, as in AD patients, the relationship is disturbed and the correlation is instead found between total retinal IAPP and total hippocampal IAPP (i.e., the value of both modified and unmodified IAPP). If this hypothesis holds true, our study adds to the increasing number of studies suggesting that AD-related pathological changes in the brain can be mirrored in the retina (Hart et al., 2016).

Interestingly, a recent preclinical study, using a double-transgenic mouse model expressing both the human Aβ precursor protein (APP) and human IAPP, has shown pancreatic accumulation of human Aβ only in the presence of amyloidogenic human IAPP (Wijesekara et al., 2017). In view of this finding, it can be speculated that IAPP is associated with the formation of Aβ depositions also in the retina. Such a cross-seeding/co-deposition hypothesis can only be verified by immunohistochemical analysis. Unfortunately, we have not been able to perform reliable staining of IAPP and Aβ due to high background and melanin contamination, which were not conquered despite several different staining protocols (including antigen retrieval and bleaching), tissue preparation (whole mount and cross-sectioning), as well as antibodies and dyes (Congo red, Thioflavin S).

We have previously, by the use of both in vitro and brain tissue studies, shown that brain pericytes internalize IAPP, leading to toxic intracellular inclusions. Moreover, Despa et al. have recently demonstrated IAPP depositions in the small vessels and capillaries in the dorsolateral frontal cortex of T2D patients with AD. They have further showed that rats overexpressing human amyloidogenic IAPP show inclusions of IAPP in hippocampal capillaries and vessel

wall, where the latter was associated with enlarged perivascular space. Interestingly, the inclusions coincide with white matter rarefaction (demyelination, vacuolation, and vessel leakage) as well as impaired spatial memory (Ly et al., 2017). In view of these findings, we found it interesting to investigate whether IAPP levels are associated with alterations in the retinal pericyte numbers or vessel length. A significant reduction of pericyte numbers was noted in pure AD patients (i.e., no LB pathology), which suggests that pericyte loss in AD patients is not restricted to the brain, but occurs also in the retina of these patients (Hart et al., 2016). The number of retinal pericytes correlated with the number of hippocampal pericytes in NCs, but not in AD patients, which might be explained by differences in time and compartments. This idea is supported by a study demonstrating Aβ accumulation in the retina before Aβ plaques appear in the brain (Koronyo-Hamaoui et al., 2011). Interestingly, we found a positive correlation between number of retinal pericytes and total unmodified IAPP ($S_{L\text{-}FA}$) levels in AD patients. This finding suggests a beneficial role for unmodified IAPP on the pericyte population. On the contrary, unmodified IAPP appeared to have an inhibiting impact on angiogenesis, as vessel length in both retina and hippocampus appeared to decrease along with increased total unmodified IAPP levels. These findings should be viewed from the perspective that defective vessels and pathological angiogenesis have been seen in both animal models of AD (Nakajima et al., 2003) and AD patients (Kalaria, 1992). Notably, although our results suggest a role for unmodified IAPP in the vascular compartment, they do not unveil whether there is a specific association between aggregated IAPP and vascular alterations as described by Despa et al. (Jackson et al., 2013; Ly et al., 2017). We found no correlation between IAPP values in the ultracentrifuged pellet fractions ($P_{U\text{-}FA}$ or $P_{U\text{-}FA\text{-}G}$) and pericyte variables or vessel length, but we cannot exclude the possibility that values of solely modified IAPP in these fractions correlates with the same.

Importantly, it should be noted that there are limitations within our study. The cohort size is small and therefore studies on larger cohorts are needed to confirm our results. Furthermore, owing to the lack of reliable immunohistochemical stainings of the retina, we have not been able to investigate the cellular localization of IAPP or its potential association with pericytes or vessels in the retina. Finally, shortage of clinical data on variables related to IAPP secretion and amyloidogenicity (such as blood glucose and cholesterol levels) limits our possibilities to draw wider conclusions on the role of IAPP in AD pathology.

5. Conclusions

To conclude, we here for the first time demonstrate the presence of IAPP in the human retina and altered unmodified IAPP levels in the AD retina. We also show an association between unmodified IAPP and pericyte numbers in retina as well as decreased angiogenesis along with increased unmodified IAPP levels in retina and hippocampus, suggesting IAPP to play a regulatory role on the vascular network. Moreover, we found a positive correlation between retinal IAPP levels and hippocampal IAPP levels, a finding supporting previous studies indicating retina as a potential window for pathological changes in the brain.

Disclosure statement

The authors declare that they have no competing interests.

Acknowledgements

The authors thank Camilla Orbjörn (Lund University) for technical support, Simon Moussaud and Henrietta M. Nielsen (Stockholm University) for apolipoprotein E genotyping and Gunilla Westermark (Uppsala University) for kindly providing the A133 antibody.

Collection of tissue and clinical data has been approved by the medical ethics review committee of VU medical center, Amsterdam, the Netherlands, and the study protocol has been approved by the regional ethical review board in Lund, Sweden. All subjects included in the study gave written informed consent.

All data generated or analyzed during this study are included in this published article.

The authors wish to thank the Swedish Research Council (M.W.), Petrus and Augusta Hedlund foundation (M.W.), Swedish Dementia foundation (M.W.), Åke Wiberg foundation (M.W.), Åhlén foundation, Segerfalk foundation (M.W.), the Crafoord foundation (M.W.), the Greta and Johan Kocks foundations (M.W.), Foundation for Old Servants (N.S.) and Stohne foundation (N.S.) for financially supporting this study. This study was accomplished while N.S. was affiliated with the Swedish National Graduate School for Competitive Science on Ageing and Health, which is funded by the Swedish Research Council.

Authors' contributions: N.S. designed the study, carried out the experiments, analyzed data and drafted the article; E.B. participated in scientific discussions and tissue preparation; NBB supplied the brain tissue, neuropathological analyses, discussions regarding tissue pretreatment, interpreting and matching clinical data, and advising on the approach of the study; M.W. designed and coordinated the study and edited the final version of the article. All authors read and approved the final article.

References

Adler, B.L., Yarchoan, M., Hwang, H.M., Louneva, N., Blair, J.A., Palm, R., Smith, M.A., Lee, H.G., Arnold, S.E., Casadesus, G., 2014. Neuroprotective effects of the amylin analogue pramlintide on Alzheimer's disease pathogenesis and cognition. Neurobiol. Aging 35, 793–801.

Banks, W.A., Kastin, A.J., Maness, L.M., Huang, W., Jaspan, J.B., 1995. Permeability of the blood-brain barrier to amylin. Life Sci. 57, 1993–2001.

Despa, S., Margulies, K.B., Chen, L., Knowlton, A.A., Havel, P.J., Taegtmeyer, H., Bers, D.M., Despa, F., 2012. Hyperamylinemia contributes to cardiac dysfunction in obesity and diabetes: a study in humans and rats. Circ. Res. 110, 598–608.

Dunkelberger, E.B., Buchanan, L.E., Marek, P., Cao, P., Raleigh, D.P., Zanni, M.T., 2012. Deamidation accelerates amyloid formation and alters amylin fiber structure. J. Am. Chem. Soc. 134, 12658–12667.

Fowler, C.B., Cunningham, R.E., O'Leary, T.J., Mason, J.T., 2007. 'Tissue surrogates' as a model for archival formalin-fixed paraffin-embedded tissues. Lab. Invest. 87, 836–846.

Frost, S., Kanagasingam, Y., Sohrabi, H., Vignarajan, J., Bourgeat, P., Salvado, O., Villemagne, V., Rowe, C.C., Macaulay, S.L., Szoeke, C., Ellis, K.A., Ames, D., Masters, C.L., Rainey-Smith, S., Martins, R.N., Group, A.R., 2013. Retinal vascular biomarkers for early detection and monitoring of Alzheimer's disease. Transl. Psychiatry 3, e233.

Fu, W., Ruangkittisakul, A., MacTavish, D., Shi, J.Y., Ballanyi, K., Jhamandas, J.H., 2012. Amyloid beta (Abeta) peptide directly activates amylin-3 receptor subtype by triggering multiple intracellular signaling pathways. J. Biol. Chem. 287, 18820–18830.

Gong, W., Liu, Z.H., Zeng, C.H., Peng, A., Chen, H.P., Zhou, H., Li, L.S., 2007. Amylin deposition in the kidney of patients with diabetic nephropathy. Kidney Int. 72, 213–218.

Hart, N.J., Koronyo, Y., Black, K.L., Koronyo-Hamaoui, M., 2016. Ocular indicators of Alzheimer's: exploring disease in the retina. Acta Neuropathol. 132, 767–787.

Hinton, D.R., Sadun, A.A., Blanks, J.C., Miller, C.A., 1986. Optic-nerve degeneration in Alzheimer's disease. N. Engl. J. Med. 315, 485–487.

Jackson, K., Barisone, G.A., Diaz, E., Jin, L.W., DeCarli, C., Despa, F., 2013. Amylin deposition in the brain: a second amyloid in Alzheimer disease? Ann. Neurol. 74, 517–526.

Jeong, H.R., An, S.S., 2015. Causative factors for formation of toxic islet amyloid polypeptide oligomer in type 2 diabetes mellitus. Clin. Interv. Aging 10, 1873–1879.

Kalaria, R.N., 1992. The blood-brain barrier and cerebral microcirculation in Alzheimer disease. Cerebrovasc. Brain Metab. Rev. 4, 226–260.

Koronyo-Hamaoui, M., Koronyo, Y., Ljubimov, A.V., Miller, C.A., Ko, M.K., Black, K.L., Schwartz, M., Farkas, D.L., 2011. Identification of amyloid plaques in retinas from Alzheimer's patients and noninvasive in vivo optical imaging of retinal plaques in a mouse model. Neuroimage 54 (Suppl 1), S204–S217.

Kwa, V.I., van der Sande, J.J., Stam, J., Tijmes, N., Vrooland, J.L. Amsterdam Vascular Medicine, Group, 2002. Retinal arterial changes correlate with cerebral small-vessel disease. Neurology 59, 1536–1540.

London, A., Benhar, I., Schwartz, M., 2013. The retina as a window to the brain-from eye research to CNS disorders. Nat. Rev. Neurol. 9, 44–53.
Ly, H., Verma, N., Wu, F., Liu, M., Saatman, K.E., Nelson, P.T., Slevin, J.T., Goldstein, L.B., Biessels, G.J., Despa, F., 2017. Brain microvascular injury and white matter disease provoked by diabetes-associated hyperamylinemia. Ann. Neurol. 82, 208–222.
Nakajima, M., Yuasa, S., Ueno, M., Takakura, N., Koseki, H., Shirasawa, T., 2003. Abnormal blood vessel development in mice lacking presenilin-1. Mech. Dev. 120, 657–667.
Oskarsson, M.E., Paulsson, J.F., Schultz, S.W., Ingelsson, M., Westermark, P., Westermark, G.T., 2015. In vivo seeding and cross-seeding of localized amyloidosis: a molecular link between type 2 diabetes and Alzheimer disease. Am. J. Pathol. 185, 834–846.
Paulsson, J.F., Westermark, G.T., 2005. Aberrant processing of human proislet amyloid polypeptide results in increased amyloid formation. Diabetes 54, 2117–2125.
Peranen, J., Rikkonen, M., Kaariainen, L., 1993. A method for exposing hidden antigenic sites in paraformaldehyde-fixed cultured cells, applied to initially unreactive antibodies. J. Histochem. Cytochem. 41, 447–454.
Qiu, W.Q., Au, R., Zhu, H., Wallack, M., Liebson, E., Li, H., Rosenzweig, J., Mwamburi, M., Stern, R.A., 2014. Positive association between plasma amylin and cognition in a homebound elderly population. J. Alzheimers Dis. 42, 555–563.
Ratnayaka, J.A., Serpell, L.C., Lotery, A.J., 2015. Dementia of the eye: the role of amyloid beta in retinal degeneration. Eye (Lond) 29, 1013–1026.
Schultz, N., Byman, E., Fex, M., Wennstrom, M., 2016. Amylin alters human brain pericyte viability and NG2 expression. J. Cereb. Blood Flow Metab. 37, 1470–1482.
Sengillo, J.D., Winkler, E.A., Walker, C.T., Sullivan, J.S., Johnson, M., Zlokovic, B.V., 2013. Deficiency in mural vascular cells coincides with blood-brain barrier disruption in Alzheimer's disease. Brain Pathol. 23, 303–310.
Westermark, P., Andersson, A., Westermark, G.T., 2011. Islet amyloid polypeptide, islet amyloid, and diabetes mellitus. Physiol. Rev. 91, 795–826.
Wijesekara, N., Ahrens, R., Sabale, M., Wu, L., Ha, K., Verdile, G., Fraser, P.E., 2017. Amyloid-beta and islet amyloid pathologies link Alzheimer's disease and type 2 diabetes in a transgenic model. FASEB J. 31, 5409–5418.
Zhu, H., Wang, X., Wallack, M., Li, H., Carreras, I., Dedeoglu, A., Hur, J.Y., Zheng, H., Fine, R., Mwamburi, M., Sun, X., Kowall, N., Stern, R.A., Qiu, W.Q., 2014. Intraperitoneal injection of the pancreatic peptide amylin potently reduces behavioral impairment and brain amyloid pathology in murine models of Alzheimer's disease. Mol. Psychiatry 20, 252–262.